

Research Article: New Research | Cognition and Behavior

## The Basolateral Amygdalae and Frontotemporal Network Functions for Threat Perception

Basolateral amygdalae and frontotemporal networks

Ruud Hortensius<sup>1,2,3</sup>, David Terburg<sup>3,4</sup>, Barak Morgan<sup>5,6</sup>, Dan J. Stein<sup>7</sup>, Jack van Honk<sup>3,4,8</sup> and Beatrice de Gelder<sup>1,3</sup>

<sup>1</sup>Brain and Emotion Laboratory Department of Cognitive Neuroscience Faculty of Psychology and Neuroscience, Maastricht University, Oxfordlaan 55, EV Maastricht 6229, The Netherlands

<sup>2</sup>Cognitive and Affective Neuroscience Laboratory, Tilburg University, Warandelaan 2, LE Tilburg 5000, The Netherlands

<sup>3</sup>Department of Psychiatry and Mental Health, University of Cape Town, J-Block, Groote Schuur Hospital, Observatory, Cape Town, South Africa

<sup>4</sup>Experimental Psychology, Utrecht University, Heidelberglaan 1, CS Utrecht 3584, The Netherlands

<sup>5</sup>Global Risk Governance Program, Department of Public Law and Institute for Humanities in Africa, University of Cape Town, University Avenue, Rondebosch 7700, Cape Town, South Africa

<sup>6</sup>DST-NRF Centre of Excellence in Human Development, DVC Research Office University of Witwatersrand, York Road, Parktown, Johannesburg, South Africa

<sup>7</sup>Department of Psychiatry and Medical Research Council (MRC) Unit on Anxiety & Stress Disorders, University of Cape Town, J-Block, Groote Schuur Hospital, Observatory, Cape Town, South Africa

<sup>8</sup>Institute of Infectious Diseases and Molecular Medicine (IDM), University of Cape Town, Anzio Road, Observatory 7925, Cape Town, South Africa

DOI: 10.1523/ENEURO.0314-16.2016

Received: 17 October 2016

Revised: 19 December 2016

Accepted: 24 December 2016

Published: 23 February 2017

**Author Contributions:** R.H., D.T., D.J.S., J.v.H., and B.d.G. designed the study; D.T. and B.M. performed research; R.H., analyzed data; R.H. and D.T. contributed analytic tools, R.H., D.T., B.M., D.J.S., J.v.H., and B.d.G. wrote the paper.

**Funding:** EC | Seventh Framework Programme (FP7): 501100004963; 249858. EC | European Research Council (ERC): 501100000781; 295673. Nederlandse Organisatie voor Wetenschappelijk Onderzoek (NWO): 501100003246; VENI 451-13-004. Nederlandse Organisatie voor Wetenschappelijk Onderzoek (NWO): 501100003246; 056-24-010. South African Medical Research Council (SAMRC): 501100001322. South African Medical Research Council (SAMRC): 501100001322.

**Conflict of Interest:** Authors report no conflict of interest.

**Correspondence should be addressed to** Beatrice de Gelder, Brain and Emotion Laboratory, Department of Cognitive Neuroscience, Faculty of Psychology and Neuroscience, Maastricht University, Oxfordlaan 55, 6229 EV Maastricht, The Netherlands, Tel.: +31 43 3881437, E-mail: [b.degelder@maastrichtuniversity.nl](mailto:b.degelder@maastrichtuniversity.nl)

**Cite as:** eNeuro 2017; 10.1523/ENEURO.0314-16.2016

**Alerts:** Sign up at [eneuro.org/alerts](http://eneuro.org/alerts) to receive customized email alerts when the fully formatted version of this Accepted Manuscript is published. Accepted manuscripts are peer-reviewed but have not been through the copyediting, formatting, or proofreading process.

This is an open-access article distributed under the terms of the Creative Commons Attribution 4.0 International (<http://creativecommons.org/licenses/by/4.0>), which permits unrestricted use, distribution and reproduction in any medium provided that the original work is properly attributed.

1 **The basolateral amygdalae and frontotemporal network functions for**  
2 **threat perception**

3 Abbreviated title: Basolateral amygdalae and frontotemporal networks

4 Ruud Hortensius<sup>1,2,3</sup>, David Terburg<sup>3,4</sup>, Barak Morgan<sup>5,6</sup>, Dan J. Stein<sup>7</sup>, Jack van Honk<sup>3,4,8</sup> and  
5 Beatrice de Gelder<sup>1,3\*</sup>

6 <sup>1</sup>Brain and Emotion Laboratory, Department of Cognitive Neuroscience, Faculty of Psychology and Neuroscience, Maastricht University,  
7 Oxfordlaan 55, 6229 EV Maastricht, The Netherlands

8 <sup>2</sup>Cognitive and Affective Neuroscience Laboratory, Tilburg University, Warandelaan 2, 5000 LE Tilburg, The Netherlands

9 <sup>3</sup>Department of Psychiatry and Mental Health, University of Cape Town, J-Block, Groote Schuur Hospital, Observatory, Cape Town, South  
10 Africa

11 <sup>4</sup>Experimental Psychology, Utrecht University, Heidelberglaan 1, 3584 CS Utrecht, The Netherlands

12 <sup>5</sup>Global Risk Governance Program, Department of Public Law and Institute for Humanities in Africa, University of Cape Town, University  
13 Avenue, Rondebosch 7700, Cape Town, South Africa

14 <sup>6</sup>DST-NRF Centre of Excellence in Human Development, DVC Research Office, University of Witwatersrand, York Road, Parktown,  
15 Johannesburg, South Africa

16 <sup>7</sup>Department of Psychiatry and Medical Research Council (MRC) Unit on Anxiety & Stress Disorders, University of Cape Town, J-Block, Groote  
17 Schuur Hospital, Observatory, Cape Town, South Africa

18 <sup>8</sup>Institute of Infectious Diseases and Molecular Medicine (IDM), University of Cape Town, Anzio Road, Observatory 7925, Cape Town, South  
19 Africa

20 Author Contributions: R.H., D.T., D.J.S., J.v.H., and B.d.G. designed the study; D.T. and B.M. performed research; R.H., analyzed data; R.H. and  
21 D.T. contributed analytic tools, R.H., D.T., B.M., D.J.S., J.v.H., and B.d.G. wrote the paper.

22  
23 \* Corresponding author at:

24 Brain and Emotion Laboratory, Department of Cognitive Neuroscience, Faculty of Psychology and Neuroscience, Maastricht University,  
25 Oxfordlaan 55 6229 EV, Maastricht, The Netherlands, +31 43 3881437, b.degelder@maastrichtuniversity.nl

26

27 Word count: Abstract (237), Significance Statement (119), Introduction (747), Discussion (1708)

28 Figures: 4 / Tables: 8 / SI: 1 (Video)

29

30

31 **Acknowledgments**

32 We thank the volunteers for their participation in this study, Armin Heinecke and Minye Zhan for  
33 assistance in functional magnetic resonance imaging analyses, and the members of the Brain and  
34 Emotion Laboratory for discussion. Development of the MacBrain Face Stimulus Set was  
35 overseen by Nim Tottenham and supported by the John D. and Catherine T. MacArthur  
36 Foundation Research Network on Early Experience and Brain Development. Please contact Nim  
37 Tottenham at [tott0006@tc.umn.edu](mailto:tott0006@tc.umn.edu) for more information concerning the stimulus set. B.d.G. and  
38 R.H. were partly funded by the project TANGO. The project TANGO acknowledges the financial  
39 support of the Future and Emerging Technologies (FET) programme within the Seventh  
40 Framework Programme for Research of the European Commission, under FET-Open grant  
41 number: 249858. B.d.G. has also received funding from the European Research Council under  
42 the European Union's Seventh Framework Programme (FP7/2007-2013)/ERC grant agreement  
43 number 295673. D.T. was supported by grants from the Netherlands Organization for Scientific  
44 Research (NWO): VENI 451-13-004. D.J.S. was supported by the Medical Research Council of  
45 South Africa. J.v.H. was supported by grants from Utrecht University, the Netherlands  
46 Organization of Scientific Research (Brain and Cognition: 056-24-010), the South African  
47 MRC/DST Professional Development Program and the University of Cape Town (Brain  
48 Behavior Initiative).

49

50 Conflict of Interest: Authors report no conflict of interest

51

52

53 **Abstract**

54 While the amygdalae play a central role in threat perception and reactions, the direct  
55 contributions of the amygdalae to specific aspects of threat perception, from ambiguity resolution  
56 to reflexive or deliberate action, remain ill understood in humans. Animal studies show that a  
57 detailed understanding requires a focus on the different subnuclei which is not yet achieved in  
58 human research. Given the limits of human imaging methods, the crucial contribution needs to  
59 come from individuals with exclusive and selective amygdalae lesions. The current study  
60 investigated the role of the basolateral amygdalae and their connection with associated frontal  
61 and temporal networks in the automatic perception of threat. Functional activation and  
62 connectivity of five individuals with Urbach-Wiethe disease with focal basolateral amygdala  
63 damage and 12 matched controls were measured with fMRI while they attended to the facial  
64 expression of a threatening face-body compound stimuli. Basolateral amygdala damage was  
65 associated with decreased activation in the temporal pole, but increased activity in the ventral and  
66 dorsal medial prefrontal and medial orbitofrontal cortex. This dissociation between the prefrontal  
67 and temporal networks was also present in the connectivity maps. Our results contribute to a  
68 dynamic, multi-role, subnuclei-based perspective on the involvement of the amygdalae in fear  
69 perception. Damage to the basolateral amygdalae decreases activity in the temporal network,  
70 while increasing activity in the frontal network thereby potentially triggering a switch from  
71 resolving ambiguity to dysfunctional threat signaling and regulation, resulting in hypersensitivity  
72 to threat.

73

74

75 **Significance statement**

76 Humans are experts in recognizing potential threat signals. While the role of the human  
77 amygdalae is widely acknowledged, the contributions of the different amygdalae nuclei and  
78 associated neural networks in threat perception remain poorly understood. Here we investigate  
79 the importance of the basolateral amygdalae and their connections with temporal and frontal  
80 regions during the processing of task-irrelevant threatening bodily signals. We tested five  
81 individuals with selective basolateral amygdalae damage. The results show that after basolateral  
82 amygdalae damage activity was increased in the frontal network but decreased in the temporal  
83 network. Together with anomalous activity in regions important for action, these results point to a  
84 disruption along three axes during threat perception, namely ambiguity resolution, safety  
85 signaling, and action preparation.

86 Keywords: amygdalae, threat, emotion, basolateral amygdalae, Urbach-Wiethe disease

87

## 88 Introduction

89 It is widely acknowledged that the amygdalae (AMG) play a central role in threat processing.  
90 Neuroimaging studies in healthy individuals have shown that the AMG are activated in response  
91 to seeing facial expressions (Morris et al., 1996; see Sabatinelli et al., 2011 for a review) as well  
92 as bodily expressions of threat (Hadjikhani and de Gelder, 2003; see de Gelder et al., 2012 for a  
93 review). However, in humans our understanding remains patchy and the specific contribution to  
94 different aspects of threat perception, from ambiguity resolution, to safety signaling and action,  
95 cannot yet be disentangled. For a better understanding of the central role of the AMG in threat  
96 perception, it is essential to distinguish the role of its different nuclei and map their specific  
97 connectivity profile (Hortensius et al., 2016a). Given the limitations of human imaging methods,  
98 the contribution of lesion studies is crucial (Adolphs, 2016; Madarasz et al., 2016).

99 The major division of the AMG is between the superficial (SFA), basolateral (BLA), and  
100 central-medial amygdalae (CMA) (McDonald, 1998). This subdivision corresponds to three  
101 different networks, the olfactory network (SFA), the autonomic network (CMA), and the frontal-  
102 temporal network (BLA) (Swanson and Petrovich, 1998; Bzdok et al., 2013). The latter two  
103 networks are specifically important for threat processing and behavior. The CMA mediate  
104 reflexive reactions to threat together with the hypothalamus and brainstem (Mosher et al., 2010;  
105 Fox et al., 2015). The role of the BLA in threat perception and action is more complex. The BLA  
106 receive input from the sensory thalamus and sensory cortices and have bidirectional connections  
107 with many cortical, including frontal and temporal, regions such as the ventral and dorsal part of  
108 medial prefrontal cortex (MPFC) and temporal pole (TP) (Heimer et al., 1997; Ghashghaei and  
109 Barbas, 2002). The BLA-temporal network plays a role in the emotional labeling of ambiguous  
110 object categories and in affective value calculation (Benarroch, 2015). The connections with the

111 medial and orbital part of the prefrontal cortex underlies safety signaling, emotion regulation and  
112 affective learning (Likhnik and Paz, 2015). The BLA are crucial in the perception and reaction to  
113 facial and bodily expressions and are particularly sensitive to ambiguity (Madarasz et al., 2016),  
114 this might especially be the case during a possible mismatch between these expressions.

115       Information from the face and the body is sampled and combined at an early stage, around  
116 115ms post-stimulus onset (Meeren et al., 2005). Bodily expressions influence recognition of  
117 facial expressions (Meeren et al., 2005; Van den Stock et al., 2007; Aviezer et al., 2008; 2012a;  
118 2012b), face identity recognition (Van den Stock and de Gelder, 2014) and memory (Van den  
119 Stock and de Gelder, 2012). For instance, the interpretation of a happy face combined with an  
120 angry body can be biased towards the latter (Kret and de Gelder, 2013). Recent behavioral  
121 evidence showed a crucial role of the BLA in the integration of face-body information. Three  
122 individuals with bilateral BLA damage showed a deficit in ignoring task-irrelevant threatening  
123 bodily expressions during emotion face recognition (de Gelder et al., 2014). The question  
124 remains how the BLA together with the temporal and frontal networks process task-irrelevant  
125 bodily threat signals and how activity in these networks changes after BLA damage.

126       In the present functional magnetic resonance imaging (fMRI) study, we investigated the  
127 neural basis of perceiving threatening facial and bodily expressions either in isolation, or in  
128 congruent (matching) or incongruent (mismatching) face-body compounds in five participants  
129 with specific BLA calcification and 12 matched controls. The goal of our study was to clarify the  
130 effect of BLA damage on activity in the frontal and temporal networks during irrelevant threat  
131 processing. The previously reported behavioral finding of excessive influence of task-irrelevant  
132 and unattended bodily expressions on facial expression recognition after BLA damage could be  
133 the result of disruption in the BLA-frontal or the BLA-temporal network and point either to a

134 mechanism rooted in threat signaling, or emotion integration and interpretation respectively, or a  
135 combination. The BLA, by activating inhibitory neurons in the MPFC, have an inhibitory  
136 influence on the MPFC (Dilgen et al., 2013), and damage to the BLA might result in an increase  
137 in activation in both the dorsal and ventral part of the MPFC. In contrast, it has been reported that  
138 long-term damage to the entire AMG resulted in structural changes in visual and temporal  
139 regions (Boes et al., 2012). BLA damage will most likely also disrupt activity in the BLA-  
140 temporal network but the exact functional consequences are at present unknown (Vuilleumier et  
141 al., 2004; Edmiston et al., 2013).

142

## 143 **Materials and Methods**

### 144 *Participants*

145 Five volunteers with Urbach-Wiethe disease (UWD) disease from the Northern Cape of South-  
146 Africa (Thornton et al., 2008) and 12 matched controls from the same region participated in the  
147 present experiment (all women). Participants had no history of secondary psychopathology or  
148 epileptic insults. Environmental conditions, age, and neuropsychological characteristics were  
149 similar for the UWD and control group (**Table 1**). UWD is a disease that in some cases includes  
150 bilateral calcification of the AMG. See **Figure 1** and **Movie 1** for the location and size of the  
151 calcification and three-dimensional reconstruction of the lesion. Previously, structural and  
152 functional MRI assessment by means of cytoarchitectonic-probability labeling provided evidence  
153 that the calcification is restricted to the BLA (Terburg et al., 2012; Klumpers et al., 2015b). Three  
154 of the five individuals with UWD (UWD 1-3) also participated in the previously reported  
155 behavioral experiment (de Gelder et al., 2014) using a design similar to the one used in the



156 present study. The three individuals with UWD showed a large and significant deficit in ignoring  
157 task-irrelevant bodily threat compared with controls (effect size ( $r$ )  $\geq$  -.58). Participants were  
158 unaware of the aim of the study and provided written informed consent. The study was approved  
159 by the Health Sciences Faculty Human Research Ethics Committee of the University of Cape  
160 Town and carried out in accordance with the standards set by the Declaration of Helsinki.

161

### 162 *Stimuli and Task*

163 Compound stimuli were created by combining facial and bodily expressions (Meeren et al.,  
164 2005). Fearful and happy faces (MacBrain Face Stimulus Set) were paired with a fearful or happy  
165 body (de Gelder and Van den Stock, 2011), resulting in congruent (e.g., a fearful face with a  
166 fearful body) or incongruent (e.g., a happy face with a fearful body) compounds. To create  
167 compound stimuli showing only facial or bodily expressions, the face or body were replaced with  
168 a grey shape (e.g., a happy face with grey rectangle, a grey oval with a fearful body). An  
169 additional control compound stimulus was created in which both facial and bodily expressions  
170 were replaced by a grey oval and grey rectangle. We used grey shapes instead of neutral  
171 expressions, as neutral expressions are often not perceived as neutral and are evaluated on  
172 multiple dimensions (Todorov et al., 2008), for example dominance (Mignault and Chaudhuri,  
173 2003; Oosterhof and Todorov, 2008), and emotion (Malatesta et al., 1987; Said et al., 2009), and  
174 the processing of these faces is influenced by the rest of the body (Van den Stock and de Gelder,  
175 2012; 2014). Ten unique stimuli (five female) per condition were created.

176 Participants performed a passive oddball task (Carretié et al., 2004). In this task,  
177 participants focused on the fixation cross placed on the nose of the face. Thus, attention of the

178 participants was on the face and not on the rest of the body. During the task an oddball stimulus  
179 could appear that would have a red circle overlaid on the nose of the face instead of a black  
180 fixation cross. Participants were instructed to pay attention to this change, but did not have to  
181 make an overt response. This was done to counteract any possible contamination of the blood-  
182 oxygenation-level dependent signal (BOLD) by a motor response. A nurse familiar to the  
183 participants was trained to provide instructions outside of the scanner. The task was explained to  
184 the participant with examples of face-body compound stimuli not used in the actual experiment.  
185 The experiment started when participants indicated that they understood the instructions.

186         A block design was used. During a stimulation block the 10 stimuli belonging to the same  
187 category (e.g., fearful face with a happy body) were presented in a random order for 800 ms each,  
188 with an inter stimulus interval of 200 ms (total duration 10 s). Each run consisted of 27  
189 stimulation blocks (nine different conditions repeated three times) and six oddball blocks  
190 presented in a random order. This was followed by an inter block interval of 6 s. Three rest  
191 blocks of 10 s each were presented at a fixed time point (after stimulation/oddball block 5, 11,  
192 and 22). To counteract any possible habituation and provide a more dynamic presentation no  
193 stimuli were shown during these rest blocks. Participants completed two runs, lasting 18 minutes  
194 in total. Stimuli were presented using E-Prime 2.0 software (Psychology Software Tools,  
195 Pittsburgh, PA, USA), projected onto a screen located at the end of the scanner bore. Each new  
196 event was synchronous with a new scan volume.

197

198

199

200 *Image acquisition*

201 Data were acquired with a Siemens Magnetom Allegra 3 Tesla head-only scanner (Siemens  
202 Medical Systems GmbH, Erlangen, Germany) at the Cape Universities Brain Imaging Centre  
203 (CUBIC) in Cape Town, South Africa. Participants were fitted with earplugs to attenuate the  
204 scanner noise and padding was used to reduce head movements. Functional whole brain coverage  
205 was achieved using 2D echo-planar images sequence. Each volume contained 36 slices acquired  
206 in ascending order with a 3.5 mm isotropic resolution (interslice gap = 0.525, TR = 2000ms, TE  
207 = 27 ms, flip angle = 70°, field of view (FOV) = 225 x 225 mm<sup>2</sup>, matrix size = 64 x 64). In total  
208 278 functional volumes were collected per run. After the final functional run a high-resolution  
209 T1-weighted anatomical scan with 1 mm isotropic resolution was collected (no gap, TR = 2300  
210 ms and TE = 39 ms, FA = 9°, field of view = 240 x 256 mm<sup>2</sup>, matrix size = 256 x 256).

211

212 *Functional magnetic resonance imaging preprocessing and analyses*

213 Data preprocessing and analyses were carried out using BrainVoyager QX Version 2.8.4 (Brain  
214 Innovation, The Netherlands, [www.brainvoyager.com](http://www.brainvoyager.com)). The first four volumes of each run were  
215 discarded from analyses to avoid T1 saturation effects. Preprocessing of the functional data  
216 consisted of slice time correction (using sinc interpolation), a rigid-body algorithm to correct for  
217 small movements between scan (trilinear/sinc estimation and interpolation), and temporal high-  
218 pass filtering (GLM-Fourier with two cycles sine/cosine per run including linear trend removal).  
219 No spatial smoothing was used. Functional data was co-registered to the anatomical data, and all  
220 data was normalized into Talairach space.

221 To reduce individual macro-anatomical differences between participants and crucially  
222 between the UWD and control group, and to subsequently improve statistical power, Cortex-  
223 Based alignment was used (Goebel et al., 2006; Frost and Goebel, 2012). This high-resolution  
224 cortical mapping procedure achieves a non-rigid alignment of different brains using the  
225 individual curvature information that reflects the gyri and sulci folding patterns (see Frost and  
226 Goebel, 2012 for more details). As the CBA procedure already applies smoothing to the data and  
227 results in superior alignment between participants, no further spatial smoothing was used.

228 At the single-subject level, a fixed-effects whole-brain general linear model was applied  
229 with each condition and oddball block defined as predictors. The z-transformed motion predictors  
230 were included as predictors of no interest. In addition, to reduce error variance, outlier predictors  
231 were included in the model (Luo and Nichols, 2003; Carter et al., 2008). An outlier map was  
232 created for each run of each participant to show clusters that have a time course value of  $> 6$  SD  
233 above the mean. The clusters in these maps were manually inspected and if the value was  $> 6$  SD  
234 above the mean, but not related to motion or an incidental spike, the time course was extracted, z-  
235 transformed, and included in the design matrix. Next, the design matrix of each run of each  
236 participant was checked and corrected for shared variance. Predictors of no interest explained by  
237 a combination of other predictors ( $R^2 > .80$ ) were removed from the design matrix. For example,  
238 if Y rotation estimates were explained by the other (motion) predictors, Y rotation estimates were  
239 not included in the model. Thus, besides the task predictors (nine + one oddball), motion  
240 predictors and possible outlier predictors were included in the design matrix. The number of  
241 predictors of no interest did not differ between groups,  $p$ 's  $> .22$ , and ranged between five and  
242 nine across subjects.

243 At the group level a random-effects general linear model was applied. Using a dummy-  
244 coded general linear model the following main analyses were performed:

- 245 1. We first investigated the regions that were activated more for fearful compared to  
246 happy bodies regardless of the facial information.
- 247 2. To map the effect of incongruent versus congruent face-body compounds we  
248 contrasted incongruent (fearful face and a happy body, and happy face and a fearful  
249 body) with congruent (fearful face and a fearful body, and happy face and a happy  
250 body).
- 251 3. To determine the influence of task-irrelevant fear versus task-irrelevant happiness,  
252 fearful bodies with a happy face or grey oval were contrasted with happy bodies with  
253 fearful face or grey oval.

254 Between-group as well as within-group (for the UWD and control group separate as well as  
255 combined) maps were calculated. The between-group maps were cluster size corrected (Forman  
256 et al., 1995). In brief, a whole-brain correction was calculated by estimating a false-positive rate  
257 for each cluster by taking into account the spatial smoothness of the initial statistical map. In  
258 accordance with Goebel, Esposito and Formisano (2006), the initial single voxel threshold was  
259 set at  $p = .01$ , and the minimal cluster size threshold applied to the final statistical maps after  
260 Monte-Carlo simulation (1000 iterations) corresponds to a cluster-level false-positive rate ( $\alpha$ ) of  
261 5%. While it has been argued that an initial threshold of  $p = .001$  is recommended (Woo et al.,  
262 2014), we chose a more liberal threshold given the special population and methodological steps  
263 (CBA, random-effects general linear model, no spatial smoothing). A more lenient threshold is  
264 advised to avoid type II errors and counteract activation pattern biases (large versus small effects  
265 and dominance of visual regions) (Lieberman and Cunningham, 2009). The individual and

266 combined group maps of the UWD and control groups were tested against zero using a one-  
267 sample t-test and thresholded at  $p < .01$ , with an extended cluster size of 25.

268       Next to testing for differences in functional segregation we established differential  
269 functional integration by performing connectivity analyses (Price et al., 2006). We used  
270 psychophysiological interaction (Friston et al., 1997) to probe the potential impact of BLA  
271 damage on the neural network underlying threat perception. Functional coupling between the  
272 seed region identified in the between-group analyses and other regions was estimated as a  
273 function of the psychological context. The demeaned extracted time course from the seed region  
274 (the physiological state) was used to create psychophysiological interaction predictors by  
275 multiplying it with the contrast of interest (psychological state). Besides psychophysiological  
276 interaction and contrast predictors, the time course of the seed region, motion, and possible  
277 outlier predictors were included in the model. After the fixed-effects single-subject analysis, a  
278 whole-brain random effects group analysis was used to map the difference in connectivity pattern  
279 between the UWD and control group. Thresholds were similar as in the functional activation  
280 analyses. All statistical maps are shown on the average group-aligned surface reconstruction and  
281 Talairach coordinates and  $t$ - and  $p$ -values of peak vertices are reported.

282

## 283 **Results**

### 284 *Functional activation*

285 No between-group differences were found when contrasting emotional faces or bodies versus  
286 control stimuli. **Tables 2** and **3** report the significant clusters for the UWD and control group  
287 combined. No significant clusters were found between- or within-groups for fearful versus happy

288 facial expression regardless of bodily expression. These functional maps are in line with previous  
289 research on face and body perception (van de Riet et al., 2009; de Gelder et al., 2010; Kret et al.,  
290 2011; Sabatinelli et al., 2011). Moreover, the lack of significant differences in functional  
291 activation between individuals with UWD and controls when perceiving emotional faces and  
292 bodies in isolation is in line with behavioral observations of intact emotion recognition of both  
293 facial and bodily expressions in isolation (Terburg et al., 2012; de Gelder et al., 2014).

294 To add to behavioral and EEG studies on face-body compound perception (Meeren et al.,  
295 2005; Kret and de Gelder, 2013; de Gelder et al., 2014) and to establish the functional activation  
296 in the presence of functional BLA, we report the functional maps in the control group separately  
297 (**Table 4-6**). Results revealed no regions that were activated more for fearful compared to happy  
298 bodies regardless of the facial information. Second, the right temporal pole (TP; Brodmann Area  
299 (BA) 21), superior (BA 38) and inferior temporal gyrus (BA 20) were activated for happy versus  
300 fearful bodies regardless of the facial information. Third, significant clusters were observed for  
301 congruent (fearful face with a fearful body or happy face with a happy body) versus incongruent  
302 face-body compounds (fearful face with a happy body or happy face with a fearful body), but not  
303 for the inverse contrast. Activity increased for congruent compared to incongruent compounds in  
304 the superior frontal gyrus (BA 6), and ventromedial prefrontal cortex (vMPFC; BA 10). Lastly,  
305 we tested the specific effect of task-irrelevant fearful versus happy bodies, that is fearful bodies  
306 combined with a happy face or a grey oval versus happy bodies with fearful faces or a grey oval.  
307 For this contrast the cingulate gyrus (BA 23) and cuneus (BA 18) were activated for task-  
308 irrelevant fear bodies compared to task-irrelevant happy bodies.

309 Next we investigated between group differences in brain regions that showed differential  
310 activation for fearful versus happy bodies. Individuals with UWD compared to controls showed

311 less activation in the left fusiform gyrus (BA 19) but more activation for fearful versus happy  
312 bodies in the right anterior part of the inferior parietal lobule (IPL; BA 40). Directly comparing  
313 incongruent with congruent face-body compounds revealed that individuals with UWD compared  
314 to controls showed more activation in the medial orbitofrontal cortex (mOFC; BA 11),  
315 ventromedial prefrontal cortex (vMPFC; BA 10), and the dorsal medial prefrontal cortex  
316 (dMPFC; BA 9). However, individuals with UWD compared to controls showed less activation  
317 in the left (BA 38) and right TP (BA 21). No significant between-group differences were found  
318 when directly contrasting task-irrelevant fear bodies versus task-irrelevant happy bodies. The  
319 results are presented in **Figure 2-4** and **Table 7**.

320 We ran an alternative analysis that focused solely on subcortical activation after BLA  
321 damage. To allow a fine-grained analysis we ran the same contrasts as in the main analyses but  
322 masked the subcortical areas. No significant clusters emerged even with spatial smoothing (4mm  
323 Gaussian kernel).

#### 324 *Functional connectivity*

325 In a first analysis, we identified regions that showed functional connectivity with the IPL and the  
326 fusiform gyrus during the processing of fearful versus happy body regardless of the facial  
327 information. This revealed increased functional connectivity between the IPL and the subgenual  
328 anterior cingulate cortex (ACC; BA 24) in individuals with UWD compared to controls.  
329 Increased coupling between the fusiform gyrus and the anterior IPL (BA 40) was observed in  
330 individuals with UWD compared to controls, highlighting the importance of the latter region in  
331 threat processing.



332           Next, we established regions that showed functional connectivity with the mOFC,  
333 vMPFC, dMPFC and left and right TP, during the processing of incongruent versus congruent  
334 face-body compounds. Interestingly, individuals with UWD compared to controls showed  
335 decreased coupling between the mOFC and the posterior IPL (BA 7). Increased functional  
336 connectivity between the cuneus (BA 19), as well as the precuneus (BA 31), with the vMPFC  
337 was observed in individuals with UWD compared to controls. With the dMPFC as seed region,  
338 individuals with UWD compared to controls showed increased coupling with the vMPFC (BA  
339 10), but decreased coupling with the superior temporal gyrus (BA 22) and TP (BA 38). Lastly,  
340 individuals with UWD compared to controls showed increased functional connectivity between  
341 the right TP and the inferior temporal gyrus (BA 20) and bilateral middle temporal gyrus (BA 21  
342 and 22), and decreased functional connectivity between the left TP and mOFC (BA 11) and  
343 superior frontal gyrus (BA 6). **Figures 2-4** and **Table 8** report the results from the functional  
344 connectivity analyses.

345

## 346 **Discussion**

347 We investigated the effects of BLA damage on activity in the frontal and temporal networks  
348 during irrelevant threat processing. Results showed that BLA damage resulted in a differential  
349 impact on the BLA-frontal network and BLA-temporal network. In the BLA-damaged group  
350 compared to control group, activity was increased for incongruent threatening face-body  
351 compounds in frontal midline regions (mOFC, vMPFC, dMPFC), but decreased in the bilateral  
352 TP. Functional connectivity analyses provided further indication of this differential effect and  
353 showed reduced coupling between frontal and temporal regions after BLA damage. Reduced

354 coupling between the dMPFC and TP and superior temporal gyrus during the perception of  
355 incongruent threatening face-body compounds was observed in individuals with BLA damage  
356 compared to controls. Under similar conditions, we also observed decreased functional  
357 connectivity after BLA damage between the left TP and mOFC and superior frontal gyrus. In  
358 addition to the impact on frontal and temporal networks, results showed changes in IPL activity  
359 after BLA damage. We observed that activation for fearful versus happy bodily expression was  
360 increased in the IPL but decreased in the fusiform gyrus in BLA-damaged compared to control  
361 individuals. Importantly, the IPL showed increased coupling with the subgenual ACC, while the  
362 fusiform gyrus showed increased functional connectivity with the IPL in the BLA-damaged  
363 compared to control group. Taken together our results reveal the impact of BLA damage on a  
364 PFC-TP-IPL network during the processing of threat. This proposed PFC-TP-IPL network may  
365 be involved in several important processes that regulate confrontations with threat along three  
366 different axes, from ambiguity resolution to safety signaling and emotion regulation to the  
367 selection and execution of actions. Damage to the BLA could result in anomalous activity in all  
368 three nodes of the network and explain the previously observed hypersensitivity to threat  
369 (Terburg et al., 2012; de Gelder et al., 2014). We now discuss these effects and the influence of  
370 BLA damage in more details.

### 371 **Temporal Pole**

372 Our results are consistent with existing knowledge on afferent and efferent connections and the  
373 functional role of the TP, a polymodal association area and part of the extended limbic system  
374 (Olson et al., 2007). Connections between TP and the nearby BLA have been reported in  
375 monkeys (Aggleton et al., 1980; Ghashghaei and Barbas, 2002), and similar connections were  
376 recently demonstrated in humans using in vivo probabilistic tractography (Bach et al., 2011) and

377 meta-analytic connectivity modeling (Bzdok et al., 2013). The TP is also densely connected to  
378 midline regions, e.g., orbitofrontal cortex (Kondo et al., 2003) and the ventral, visual, part of the  
379 TP receives input from extrastriate visual areas, e.g., inferior temporal regions (Markowitsch et  
380 al., 1985).

381         In view of findings showing that the TP is activated in a variety of social emotional tasks,  
382 from face perception to theory of mind, a recent review proposed a unifying role that could  
383 underlie the variety of results (Olson et al., 2007). The authors suggested that the TP binds  
384 valence to incoming visual signals, thereby providing the affective meaning to the percept. If so,  
385 one would expect that TP also drives the emotional labeling of possible ambiguous social cues.  
386 Indeed, increased TP activity was observed when participants view unique stimuli (Asari et al.,  
387 2008), or when participants labeled the emotion of two subtly different social interactions (Sinke  
388 et al., 2010). Importantly, this proposed perception-emotion linkage is similar to the role of the  
389 BLA in emotional coloring of a signal (Benarroch, 2015).

390         The TP together with the BLA might orchestrate the coupling between emotion and  
391 perception. This BLA-TP network establishes the emotional label and biases ongoing neural  
392 processes. The decreased activation to incongruent threatening face-body compounds, i.e.  
393 ambiguous threat, in the TP and decreased coupling with the mOFC after BLA damage could  
394 potentially underlie incorrect labeling of the compound as threat and subsequently bias upstream  
395 neural activity (e.g., midline PFC). This refers to a potential perceptual bias effect in which a  
396 task-irrelevant stimulus influences the percept of the task-relevant stimulus in the direction of the  
397 former (de Gelder and Bertelson, 2003). This effect is enhanced after BLA damage (de Gelder et  
398 al., 2014), and could thus be related to dysfunctional TP functioning and reduced cross-talk

399 between temporal and frontal regions leading to impaired integration of perceptual and emotional  
400 processes.

#### 401 **Prefrontal Midline**

402 The orbital and medial parts of the prefrontal midline that showed increased activation in the  
403 BLA-damaged group during incongruent or ambiguous threat are strongly connected to the BLA  
404 (Barbas, 2015) and have consistently been implicated in social-emotional processes (Likhtik and  
405 Paz, 2015). However, the different parts of the prefrontal midline have different connectivity  
406 patterns with regions within the AMG and have distinct but related roles (Barbas et al., 2003;  
407 Ghashghaei et al., 2007). Different functional consequences can emerge based on the precise  
408 location of the disruption in these amygdalae-prefrontal pathways (Myers-Schulz and Koenigs,  
409 2012; Grupe and Nitschke, 2013). A disruption in the BLA-orbitofrontal pathway can lead to  
410 increased threat attention and hypervigilance (van Honk et al., 2016). On the other hand,  
411 disruption in the inhibitory control of the vMPFC on the BLA is thought to result in impaired  
412 safety learning (Grupe and Nitschke, 2013), consistent with the role of the MPFC-BLA pathway  
413 in safety signaling (Likhtik and Paz, 2015). This would hold especially for the ventral part of the  
414 MPFC, as the dorsal part has been associated with threat anticipation (Grupe and Nitschke, 2013;  
415 Klumpers et al., 2015a). For instance, when participants are confronted with a real-life threat and  
416 overcame their fear, vMPFC activation increased and was positively related to subjective fear  
417 (Nili et al., 2010). As the basolateral nuclei are central to these prefrontal pathways, damage to  
418 the BLA could lead to both hypervigilance to threat (Terburg et al., 2012) and impairment in  
419 safety signaling by increased attention to irrelevant threat (de Gelder et al., 2014).

420 Most often threat signals are congruent and unambiguous but sometimes the relevance  
421 and the actual threat significance of one cue conflicts with that of another and/or the  
422 interpretation of the context. The importance of the AMG, in particular the BLA, and the MPFC  
423 in these processes has been reported (Kim et al., 2003; Etkin et al., 2004; Kim et al., 2004; Etkin  
424 et al., 2006; Brand et al., 2007; Neta et al., 2013; Nohlen et al., 2014). For example, the BLA  
425 code the subjective interpretation of the emotion of the face (Wang et al., 2014). Interestingly,  
426 when participants are interpreting ambiguous emotional faces MPFC and BLA activation are  
427 inversely correlated (Kim et al., 2003). Similar findings of distraction by irrelevant threat (de  
428 Gelder et al., 2014) and increased reactivity to negative social emotional signals found after BLA  
429 damage (Terburg et al., 2012) have been obtained in individuals with mood and anxiety disorders  
430 (Mathews and MacLeod, 1994). Related to this, changes in connectivity of the MPFC with (parts  
431 of) the AMG have been found after early life stress (Malter Cohen et al., 2013), trauma  
432 (Thomason et al., 2015) and general anxiety disorder (Greenberg et al., 2013; Roy et al., 2013).  
433 Deficits in threat discrimination have been related to less differential responses in the vMPFC  
434 (Greenberg et al., 2013) and to decreased MPFC-AMG connectivity (Cha et al., 2014). The  
435 absence of BLA input to the MPFC may lead to dysfunctional threat signaling and threat  
436 regulation.

#### 437 **Inferior Parietal Lobule**

438 Increased activation in the IPL for fearful bodily expressions regardless of the facial information  
439 was found after BLA damage. Moreover, under the same task conditions increased coupling  
440 between the fusiform gyrus and IPL was observed in the BLA-damaged compared to the control  
441 group. The IPL has been implicated in action observation and representation (Rizzolatti and  
442 Matelli, 2003), maintaining attention (Malhotra et al., 2009), and fear processing (de Gelder et

443 al., 2004; Sinke et al., 2010; Becker et al., 2012; Engelen et al., 2015). Several observations in the  
444 literature point to a possible link between the IPL and the representation and preparation of action  
445 during threat and the influence of the AMG on these processes. The right IPL has been implicated  
446 in responding to salient information in the environment (Singh-Curry and Husain, 2009). Directly  
447 influencing IPL activity during emotion body perception using online Transcranial Magnetic  
448 Stimulation resulted in increased sensitivity for fearful bodily expressions (Engelen et al., 2015).  
449 A study that investigated face processing in two patients with complete bilateral AMG damage,  
450 showed that the one patient that had both intact recognition of fearful facial expressions and  
451 startle responses to negative pictures also had increased activation in the premotor cortex and the  
452 IPL to fearful faces (Becker et al., 2012). In a recent study with the same population as in the  
453 present study, a ventral-to-dorsal processing shift during contextualized threat perception was  
454 observed after BLA damage (Hortensius et al., 2016b). Increased activation was observed in the  
455 anterior part of the IPL and other regions in the dorsal stream during the perception of neutral  
456 faces in a threatening scene. In the presence of BLA damage, a dorsal route instead of a ventral  
457 route, might dominate the processing of task-irrelevant threat probing reflexive reactions to threat  
458 (de Gelder et al., 2012). However, the IPL is a heterogeneous region and encompasses as much as  
459 five different clusters (Mars et al., 2011), each with distinctive roles (for example Kwok and  
460 Macaluso, 2015). In the present study both the anterior and posterior IPL were implicated in the  
461 neural circuitry after BLA damage, but under different task conditions and in different  
462 hemispheres. The anterior region is connected to premotor cortex and could serve as a crucial hub  
463 in the transition from perception to action. In contrast, the posterior part of the IPL is connected  
464 to the parahippocampal gyrus and activated during memory tasks. Which exact roles these  
465 different regions fulfill during threat perception and how these functional profiles change after  
466 BLA damage is unknown.

467 **Conclusion**

468 To conclude, our study is the first to show the significance of a PFC-TP-IPL network in the  
469 functional integration of and reaction to threatening social stimuli by using a unique sample of  
470 individuals with BLA damage. Rather than attributing a function to the amygdala as a whole, we  
471 clarify the specific contribution of one of its major nuclei in automatic action preparation in the  
472 IPL, dysfunctional emotion regulation processes in the prefrontal cortex, particularly the vMPFC,  
473 and less efficient ambiguity resolution in the TP.

474

475

476 **References**

- 477 Adolphs R (2016) Human Lesion Studies in the 21st Century. *Neuron* 90:1151–1153.
- 478 Aggleton JP, Burton MJ, Passingham RE (1980) Cortical and subcortical afferents to the amygdala of the rhesus  
479 monkey (*Macaca mulatta*). *Brain Res* 190:347–368.
- 480 Amunts K, Kedo O, Kindler M, Pieperhoff P, Mohlberg H, Shah NJ, Habel U, Schneider F, Zilles K (2005)  
481 Cytoarchitectonic mapping of the human amygdala, hippocampal region and entorhinal cortex: intersubject  
482 variability and probability maps. *Anat Embryol* 210:343–352.
- 483 Asari T, Konishi S, Jimura K, Chikazoe J, Nakamura N, Miyashita Y (2008) Right temporopolar activation  
484 associated with unique perception. *Neuroimage* 41:145–152.
- 485 Aviezer H, Hassin RR, Ryan J, Grady C, Susskind J, Anderson A, Moscovitch M, Bentin S (2008) Angry, disgusted,  
486 or afraid? Studies on the malleability of emotion perception. *Psychological Science* 19:724–732.
- 487 Aviezer H, Trope Y, Todorov A (2012a) Body cues, not facial expressions, discriminate between intense positive  
488 and negative emotions. *Science (New York, NY)* 338:1225–1229.
- 489 Aviezer H, Trope Y, Todorov A (2012b) Holistic person processing: faces with bodies tell the whole story. *Journal*  
490 *of personality and social psychology* 103:20–37.
- 491 Bach DR, Behrens TE, Garrido L, Weiskopf N, Dolan RJ (2011) Deep and superficial amygdala nuclei projections  
492 revealed in vivo by probabilistic tractography. *Journal of Neuroscience* 31:618–623.
- 493 Barbas H (2015) General Cortical and Special Prefrontal Connections: Principles from Structure to Function. *Annu*  
494 *Rev Neurosci* 38:269–289.
- 495 Barbas H, Saha S, Rempel-Clower N, Ghashghaei T (2003) Serial pathways from primate prefrontal cortex to  
496 autonomic areas may influence emotional expression. *BMC Neurosci* 4:25.
- 497 Becker B, Mihov Y, Scheele D, Kendrick KM, Feinstein JS, Matusch A, Aydin M, Reich H, Urbach H, Oros-  
498 Peusquens A-M, Shah NJ, Kunz WS, Schlaepfer TE, Zilles K, Maier W, Hurlmann R (2012) Fear processing  
499 and social networking in the absence of a functional amygdala. *Biological Psychiatry* 72:70–77.
- 500 Benarroch EE (2015) The amygdala: functional organization and involvement in neurologic disorders. *Neurology*  
501 84:313–324.
- 502 Boes AD, Mehta S, Rudrauf D, Van Der Plas E, Grabowski T, Adolphs R, Nopoulos P (2012) Changes in cortical  
503 morphology resulting from long-term amygdala damage. *Social Cognitive and Affective Neuroscience* 7:588–  
504 595.
- 505 Brand M, Grabenhorst F, Starcke K, Vandekerckhove MMP, Markowitsch HJ (2007) Role of the amygdala in  
506 decisions under ambiguity and decisions under risk: evidence from patients with Urbach-Wiethe disease.  
507 *Neuropsychologia* 45:1305–1317.
- 508 Bzdok D, Laird AR, Zilles K, Fox PT, Eickhoff SB (2013) An investigation of the structural, connective, and  
509 functional subspecialization in the human amygdala. *Human brain mapping* 34:3247–3266.
- 510 Carretié L, Hinojosa JA, Martín-Loeches M, Mercado F, Tapia M (2004) Automatic attention to emotional stimuli:  
511 neural correlates. *Human brain mapping* 22:290–299.
- 512 Carter CS, Hecker S, Nichols T, Pine DS, Strother S (2008) Optimizing the design and analysis of clinical



- 513 functional magnetic resonance imaging research studies. *Biological Psychiatry* 64:842–849.
- 514 Cha J, Greenberg T, Carlson JM, Dedora DJ, Hajcak G, Mujica-Parodi LR (2014) Circuit-wide structural and  
515 functional measures predict ventromedial prefrontal cortex fear generalization: implications for generalized  
516 anxiety disorder. *Journal of Neuroscience* 34:4043–4053.
- 517 de Gelder B, Bertelson P (2003) Multisensory integration, perception and ecological validity. *Trends in cognitive*  
518 *sciences* 7:460–467.
- 519 de Gelder B, Hortensius R, Tamietto M (2012) Attention and awareness each influence amygdala activity for  
520 dynamic bodily expressions—a short review. *Front Integr Neurosci* 6:54.
- 521 de Gelder B, Snyder J, Greve D, Gerard G, Hadjikhani N (2004) Fear fosters flight: a mechanism for fear contagion  
522 when perceiving emotion expressed by a whole body. *Proceedings of the National Academy of Sciences of the*  
523 *United States of America* 101:16701–16706.
- 524 de Gelder B, Terburg D, Morgan B, Hortensius R, Stein DJ, van Honk J (2014) The role of human basolateral  
525 amygdala in ambiguous social threat perception. *CORTEX* 52:28–34.
- 526 de Gelder B, Van den Stock J (2011) The Bodily Expressive Action Stimulus Test (BEAST). Construction and  
527 Validation of a Stimulus Basis for Measuring Perception of Whole Body Expression of Emotions. *Front*  
528 *Psychol* 2:181.
- 529 de Gelder B, Van den Stock J, Meeren HKM, Sinke CBA, Kret ME, Tamietto M (2010) Standing up for the body.  
530 Recent progress in uncovering the networks involved in the perception of bodies and bodily expressions.  
531 *Neuroscience & Biobehavioral Reviews* 34:513–527.
- 532 Dilgen J, Tejada HA, O'Donnell P (2013) Amygdala inputs drive feedforward inhibition in the medial prefrontal  
533 cortex. *J Neurophysiol* 110:221–229.
- 534 Edmiston EK, McHugo M, Dukic MS, Smith SD, Abou-Khalil B, Eggers E, Zald DH (2013) Enhanced visual  
535 cortical activation for emotional stimuli is preserved in patients with unilateral amygdala resection. *Journal of*  
536 *Neuroscience* 33:11023–11031.
- 537 Eickhoff SB, Stephan KE, Mohlberg H, Grefkes C, Fink GR, Amunts K, Zilles K (2005) A new SPM toolbox for  
538 combining probabilistic cytoarchitectonic maps and functional imaging data. *Neuroimage* 25:1325–1335.
- 539 Engelen T, de Graaf TA, Sack AT, de Gelder B (2015) A causal role for inferior parietal lobule in emotion body  
540 perception. *CORTEX* 73:195–202.
- 541 Etkin A, Egner T, Peraza DM, Kandel ER, Hirsch J (2006) Resolving emotional conflict: a role for the rostral  
542 anterior cingulate cortex in modulating activity in the amygdala. *Neuron* 51:871–882.
- 543 Etkin A, Klemenhagen KC, Dudman JT, Rogan MT, Hen R, Kandel ER, Hirsch J (2004) Individual differences in  
544 trait anxiety predict the response of the basolateral amygdala to unconsciously processed fearful faces. *Neuron*  
545 44:1043–1055.
- 546 Forman SD, Cohen JD, Fitzgerald M, Eddy WF, Mintun MA, Noll DC (1995) Improved assessment of significant  
547 activation in functional magnetic resonance imaging (fMRI): use of a cluster-size threshold. *Magn Reson Med*  
548 33:636–647.
- 549 Fox AS, Oler JA, Tromp DPM, Fudge JL, Kalin NH (2015) Extending the amygdala in theories of threat processing.  
550 *Trends in Neurosciences* 38:319–329.
- 551 Friston KJ, Buechel C, Fink GR, Morris J, Rolls E, Dolan RJ (1997) Psychophysiological and modulatory

- 552 interactions in neuroimaging. *Neuroimage* 6:218–229.
- 553 Frost MA, Goebel R (2012) Measuring structural-functional correspondence: spatial variability of specialised brain  
554 regions after macro-anatomical alignment. *Neuroimage* 59:1369–1381.
- 555 Ghashghaei HT, Barbas H (2002) Pathways for emotion: interactions of prefrontal and anterior temporal pathways in  
556 the amygdala of the rhesus monkey. *Neuroscience* 115:1261–1279.
- 557 Ghashghaei HT, Hilgetag CC, Barbas H (2007) Sequence of information processing for emotions based on the  
558 anatomic dialogue between prefrontal cortex and amygdala. *Neuroimage* 34:905–923.
- 559 Goebel R, Esposito F, Formisano E (2006) Analysis of functional image analysis contest (FIAC) data with  
560 brainvoyager QX: From single-subject to cortically aligned group general linear model analysis and self-  
561 organizing group independent component analysis. *Human brain mapping* 27:392–401.
- 562 Greenberg T, Carlson JM, Cha J, Hajcak G, Mujica-Parodi LR (2013) Ventromedial prefrontal cortex reactivity is  
563 altered in generalized anxiety disorder during fear generalization. *Depress Anxiety* 30:242–250.
- 564 Grupe DW, Nitschke JB (2013) Uncertainty and anticipation in anxiety: an integrated neurobiological and  
565 psychological perspective. *Nat Rev Neurosci* 14:488–501.
- 566 Hadjikhani N, de Gelder B (2003) Seeing fearful body expressions activates the fusiform cortex and amygdala.  
567 *Current Biology* 13:2201–2205.
- 568 Heimer L, Harlan RE, Alheid GF, Garcia MM, de Olmos J (1997) Substantia innominata: a notion which impedes  
569 clinical-anatomical correlations in neuropsychiatric disorders. *Neuroscience* 76:957–1006.
- 570 Hortensius R, Terburg D, Morgan B, Stein DJ, van Honk J, de Gelder B (2016a) The dynamic consequences of  
571 amygdala damage on threat processing in Urbach-Wiethe Disease. A commentary on Pishnamazi et al. (2016).  
572 *CORTEX*.
- 573 Hortensius R, Terburg D, Morgan B, Stein DJ, van Honk J, de Gelder B (2016b) The role of the basolateral  
574 amygdala in the perception of faces in natural contexts. *Philos Trans R Soc Lond, B, Biol Sci* 371:20150376.
- 575 Kim H, Somerville LH, Johnstone T, Alexander AL, Whalen PJ (2003) Inverse amygdala and medial prefrontal  
576 cortex responses to surprised faces. *Neuroreport* 14:2317–2322.
- 577 Kim H, Somerville LH, Johnstone T, Polis S, Alexander AL, Shin LM, Whalen PJ (2004) Contextual modulation of  
578 amygdala responsivity to surprised faces. *Journal of cognitive neuroscience* 16:1730–1745.
- 579 Klumpers F, Kroes MC, Heitland I, Everaerd D, Akkermans SEA, Oosting RS, van Wingen G, Franke B, Kenemans  
580 JL, Fernández G, Baas JMP (2015a) Dorsomedial Prefrontal Cortex Mediates the Impact of Serotonin  
581 Transporter Linked Polymorphic Region Genotype on Anticipatory Threat Reactions. *Biological Psychiatry*  
582 78:582–589.
- 583 Klumpers F, Morgan B, Terburg D, Stein DJ, van Honk J (2015b) Impaired acquisition of classically conditioned  
584 fear-potentiated startle reflexes in humans with focal bilateral basolateral amygdala damage. *Social Cognitive  
585 and Affective Neuroscience* 10:1161–1168.
- 586 Kondo H, Saleem KS, Price JL (2003) Differential connections of the temporal pole with the orbital and medial  
587 prefrontal networks in macaque monkeys. *The Journal of comparative neurology* 465:499–523.
- 588 Kret ME, de Gelder B (2013) When a smile becomes a fist: the perception of facial and bodily expressions of  
589 emotion in violent offenders. *Exp Brain Res* 228:399–410.

- 590 Kret ME, Pichon S, Grèzes J, de Gelder B (2011) Similarities and differences in perceiving threat from dynamic  
591 faces and bodies. *An fMRI study. Neuroimage* 54:1755–1762.
- 592 Kwok SC, Macaluso E (2015) Exogenous features versus prior experiences modulate different subregions of the  
593 right IPL during episodic memory retrieval. *Scientific Reports* 5:11248.
- 594 Lieberman MD, Cunningham WA (2009) Type I and Type II error concerns in fMRI research: re-balancing the  
595 scale. *Social Cognitive and Affective Neuroscience* 4:423–428.
- 596 Likhtik E, Paz R (2015) Amygdala-prefrontal interactions in (mal)adaptive learning. *Trends in Neurosciences*  
597 38:158–166.
- 598 Luo WL, Nichols TE (2003) Diagnosis and exploration of massively univariate neuroimaging models. *Neuroimage*  
599 19:1014–1032.
- 600 Madarasz TJ, Diaz-Mataix L, Akhand O, Ycu EA, LeDoux JE, Johansen JP (2016) Evaluation of ambiguous  
601 associations in the amygdala by learning the structure of the environment. *Nature neuroscience* 19:965–972.
- 602 Malatesta CZ, Fiore MJ, Messina JJ (1987) Affect, personality, and facial expressive characteristics of older people.  
603 *Psychol Aging* 2:64–69.
- 604 Malhotra P, Coulthard EJ, Husain M (2009) Role of right posterior parietal cortex in maintaining attention to spatial  
605 locations over time. *Brain* 132:645–660.
- 606 Malter Cohen M, Jing D, Yang RR, Tottenham N, Lee FS, Casey BJ (2013) Early-life stress has persistent effects on  
607 amygdala function and development in mice and humans. *Proceedings of the National Academy of Sciences of*  
608 *the United States of America* 110:18274–18278.
- 609 Markowitsch HJ, Emmans D, Irle E, Streicher M, Preilowski B (1985) Cortical and subcortical afferent connections  
610 of the primate's temporal pole: a study of rhesus monkeys, squirrel monkeys, and marmosets. *The Journal of*  
611 *comparative neurology* 242:425–458.
- 612 Mars RB, Jbabdi S, Sallet J, O'Reilly JX, Croxson PL, Olivier E, Noonan MP, Bergmann C, Mitchell AS, Baxter  
613 MG, Behrens TEJ, Johansen-Berg H, Tomassini V, Miller KL, Rushworth MFS (2011) Diffusion-weighted  
614 imaging tractography-based parcellation of the human parietal cortex and comparison with human and macaque  
615 resting-state functional connectivity. *Journal of Neuroscience* 31:4087–4100.
- 616 Mathews A, MacLeod C (1994) Cognitive approaches to emotion and emotional disorders. *Annu Rev Psychol*  
617 45:25–50.
- 618 McDonald AJ (1998) Cortical pathways to the mammalian amygdala. *Progress in Neurobiology* 55:257–332.
- 619 Meeren HKM, van Heijnsbergen CCRJ, de Gelder B (2005) Rapid perceptual integration of facial expression and  
620 emotional body language. *Proceedings of the National Academy of Sciences of the United States of America*  
621 102:16518–16523.
- 622 Mignault A, Chaudhuri A (2003) The Many Faces of a Neutral Face: Head Tilt and Perception of Dominance and  
623 Emotion. *Journal of Nonverbal Behavior* 27:111–132.
- 624 Morris JS, Frith CD, Perrett DI, Rowland D, Young AW, Calder AJ, Dolan RJ (1996) A differential neural response  
625 in the human amygdala to fearful and happy facial expressions. *Nature* 383:812–815.
- 626 Mosher CP, Zimmerman PE, Gothard KM (2010) Response characteristics of basolateral and centromedial neurons  
627 in the primate amygdala. *Journal of Neuroscience* 30:16197–16207.

- 628 Myers-Schulz B, Koenigs M (2012) Functional anatomy of ventromedial prefrontal cortex: implications for mood  
629 and anxiety disorders. *Mol Psychiatry* 17:132–141.
- 630 Neta M, Kelley WM, Whalen PJ (2013) Neural responses to ambiguity involve domain-general and domain-specific  
631 emotion processing systems. *Journal of cognitive neuroscience* 25:547–557.
- 632 Nili U, Goldberg H, Weizman A, Dudai Y (2010) Fear thou not: activity of frontal and temporal circuits in moments  
633 of real-life courage. *Neuron* 66:949–962.
- 634 Nohlen HU, van Harreveld F, Rotteveel M, Lelieveld G-J, Crone EA (2014) Evaluating ambivalence: social-  
635 cognitive and affective brain regions associated with ambivalent decision-making. *Social Cognitive and  
636 Affective Neuroscience* 9:924–931.
- 637 Olson IR, Plotzker A, Ezzyat Y (2007) The Enigmatic temporal pole: a review of findings on social and emotional  
638 processing. *Brain* 130:1718–1731.
- 639 Oosterhof NN, Todorov A (2008) The functional basis of face evaluation. *Proceedings of the National Academy of  
640 Sciences of the United States of America* 105:11087–11092.
- 641 Price CJ, Crinion J, Friston KJ (2006) Design and analysis of fMRI studies with neurologically impaired patients. *J  
642 Magn Reson Imaging* 23:816–826.
- 643 Rizzolatti G, Matelli M (2003) Two different streams form the dorsal visual system: anatomy and functions. *Exp  
644 Brain Res* 153:146–157.
- 645 Roy AK, Fudge JL, Kelly C, Perry JSA, Daniele T, Carlisi C, Benson B, Castellanos FX, Milham MP, Pine DS,  
646 Ernst M (2013) Intrinsic functional connectivity of amygdala-based networks in adolescent generalized anxiety  
647 disorder. *J Am Acad Child Adolesc Psychiatry* 52:290–299.e292.
- 648 Sabatinelli D, Fortune EE, Li Q, Siddiqui A, Krafft C, Oliver WT, Beck S, Jeffries J (2011) Emotional perception:  
649 meta-analyses of face and natural scene processing. *Neuroimage* 54:2524–2533.
- 650 Said CP, Sebe N, Todorov A (2009) Structural resemblance to emotional expressions predicts evaluation of  
651 emotionally neutral faces. *Emotion* 9:260–264.
- 652 Singh-Curry V, Husain M (2009) The functional role of the inferior parietal lobe in the dorsal and ventral stream  
653 dichotomy. *Neuropsychologia* 47:1434–1448.
- 654 Sinke CBA, Sorger B, Goebel R, de Gelder B (2010) Tease or threat? Judging social interactions from bodily  
655 expressions. *Neuroimage* 49:1717–1727.
- 656 Swanson LW, Petrovich GD (1998) What is the amygdala? *Trends in Neurosciences* 21:323–331.
- 657 Terburg D, Morgan BE, Montoya ER, Hooge IT, Thornton HB, Hariri AR, Panksepp J, Stein DJ, van Honk J (2012)  
658 Hypervigilance for fear after basolateral amygdala damage in humans. *Transl Psychiatry* 2:e115.
- 659 Thomason ME, Marusak HA, Tocco MA, Vila AM, McGarragle O, Rosenberg DR (2015) Altered amygdala  
660 connectivity in urban youth exposed to trauma. *Social Cognitive and Affective Neuroscience* 10:1460–1468.
- 661 Thornton HB, Nel D, Thornton D, van Honk J, Baker GA, Stein DJ (2008) The neuropsychiatry and  
662 neuropsychology of lipid proteinosis. *J Neuropsychiatry Clin Neurosci* 20:86–92.
- 663 Todorov A, Said CP, Engell AD, Oosterhof NN (2008) Understanding evaluation of faces on social dimensions.  
664 *Trends in cognitive sciences* 12:455–460.

- 665 van de Riet WAC, Grèzes J, de Gelder B (2009) Specific and common brain regions involved in the perception of  
666 faces and bodies and the representation of their emotional expressions. *Social Neuroscience* 4:101–120.
- 667 Van den Stock J, de Gelder B (2012) Emotional information in body and background hampers recognition memory  
668 for faces. *Neurobiol Learn Mem* 97:321–325.
- 669 Van den Stock J, de Gelder B (2014) Face identity matching is influenced by emotions conveyed by face and body.  
670 *Front Hum Neurosci* 8:53.
- 671 Van den Stock J, Righart R, de Gelder B (2007) Body expressions influence recognition of emotions in the face and  
672 voice. *Emotion* 7:487–494.
- 673 van Honk J, Terburg D, Thornton HB, Stein DJ, Morgan B (2016) Consequences of selective bilateral lesions to the  
674 basolateral amygdala in humans. In: *Living without an amygdala* (Amaral DG, Adolphs R, eds). New York,  
675 NY.
- 676 Vuilleumier P, Richardson MP, Armony JL, Driver J, Dolan RJ (2004) Distant influences of amygdala lesion on  
677 visual cortical activation during emotional face processing. *Nature neuroscience* 7:1271–1278.
- 678 Wang S, Tudusciuc O, Mamelak AN, Ross IB, Adolphs R, Rutishauser U (2014) Neurons in the human amygdala  
679 selective for perceived emotion. *Proceedings of the National Academy of Sciences of the United States of*  
680 *America* 111:E3110–E3119.
- 681 Woo C-W, Krishnan A, Wager TD (2014) Cluster-extent based thresholding in fMRI analyses: pitfalls and  
682 recommendations. *Neuroimage* 91:412–419.
- 683
- 684

685

686 **Figure 1. Location and size of the BLA damage.** Coronal view of T2-weighted magnetic resonance  
687 images (left) and a three-dimensional reconstruction (middle) of the lesion for the five individuals with  
688 Urbach-Wiethe disease (UWD) with birth year indicated. Reconstruction of the AMG subnuclei was  
689 based on the cytoarchitectonic probability maps from Amunts et al. (2005) in Eickhoff et al. (2005)  
690 (right). Black rectangle indicates viewpoint for three-dimensional reconstruction.

691

692 **Figure 2. The importance of the IPL in the processing of fearful body expressions.** The UWD group  
693 showed more activation for fearful versus happy bodies in the right anterior IPL, but less activation in the  
694 left fusiform gyrus (top). Increased functional connectivity between the IPL and the subgenual ACC, and  
695 the fusiform gyrus and the anterior IPL was observed in individuals with UWD compared to controls  
696 (bottom). Purple outline indicates that the cluster survived whole-brain cluster-size correction with an  
697 initial single voxel threshold of  $p < .005$ .

698

699 **Figure 3. Enhancement of PFC midline activation during perception of incongruent threatening**  
700 **face-body compounds after BLA damage.** The mOFC, vMPFC, and dMPFC showed increased activity  
701 in the UWD group (top left) during incongruent threatening face-body compound perception. Inset shows  
702 increased dMPFC activation for incongruent versus congruent face-body compounds in individuals with  
703 UWD, and decreased vMPFC activation for the same contrast in controls. Individuals with UWD showed  
704 decreased functional connectivity between the mOFC and the posterior IPL, and increased functional  
705 connectivity between the cuneus and precuneus with the vMPFC. The dMPFC showed increased coupling  
706 with the VMPFC, but decreased coupling with the superior temporal gyrus and TP (right and bottom).  
707 Maps are cluster-size corrected except for the within-group maps that are shown with a threshold of  $p <$   
708  $.05$  uncorrected for illustration purposes. Purple outline indicates that the cluster survived whole-brain  
709 cluster-size correction with an initial single voxel threshold of  $p < .005$ .

710

711 **Figure 4. Disruption of TP in processing of incongruent threatening face-body compounds after**  
712 **BLA damage.** Activity in the TP was reduced for the UWD group during perception of incongruent  
713 threatening face-body compounds (top left). Inset shows decreased bilateral TP activation for incongruent  
714 versus congruent face-body compounds in individuals with UWD, and increased bilateral TP activation  
715 for the same contrast in controls. Consistent with the dissociation between the frontal and temporal  
716 network, increased functional connectivity was observed in individuals with UWD between the left TP  
717 and mOFC and superior frontal gyrus. The right TP showed increased coupling with the inferior temporal  
718 gyrus and bilateral middle temporal gyrus (right and bottom). Maps are cluster-size corrected except for  
719 the within-group maps that are shown with a threshold of  $p < .05$  uncorrected for illustration purposes.  
720 Purple outline indicates that the cluster survived whole-brain cluster-size correction with an initial single  
721 voxel threshold of  $p < .005$ .

722

**Table 1** Demographic data

	UWD ( <i>n</i> = 5)					Controls ( <i>n</i> = 12)	
	UWD 1	UWD 2	UWD 3	UWD 4	UWD 6	Mean	Mean
Age	27	34	38	52	39	38±9.14	37.17±5.20
VIQ	97	84	93	82	83	87.80±6.76	86.67±4.68
PIQ	99	87	85	84	87	88.40±6.07	88.17±5.39
FSIQ	98	84	87	81	83	86.60±6.73	85.83±4.43

VIQ: verbal IQ, PIQ: performance IQ, FSIQ: full-scale IQ. Means and standard deviations are reported. No significant differences between groups,  $p$ 's  $\geq .78$ .

723

**Table 2** Fearful and happy faces > control stimuli for both the UWD and control group

	Hemisphere	Talairach coordinates			Brodmann	<i>t</i>	<i>p</i>	Number of vertices
		<i>x</i>	<i>y</i>	<i>z</i>				
Inferior occipital gyrus	RH	27	-87	-9	18	6.756	.000005	183
Fusiform gyrus	RH	35	-55	-13	37	6.321	.00001	133
Lingual gyrus	RH	8	-72	4	18	5.199	.000088	39
Inferior occipital gyrus	LH	-29	-84	-7	18	8.947	<.000001	717
Middle frontal gyrus	LH	-18	18	53	6	4.924	.000153	42
Cuneus	LH	-7	-81	4	17	4.983	.000136	90
Precuneus	LH	-20	-63	49	7	4.411	.000437	76
Superior frontal gyrus	LH	-20	45	31	9	6.493	.000007	109

$p < .01$  (uncorrected) with an extended cluster size of 25. Faces are presented with a grey rectangle, and the control stimulus is a grey oval and rectangle.

724



**Table 3** Fearful and happy bodies > control stimuli for both the UWD and control group

	Hemisphere	Talairach coordinates			Brodmann	<i>t</i>	<i>p</i>	Number of vertices
		x	y	z				
Lingual gyrus	RH	15	-84	-11	18	5.323	.000069	93
Fusiform gyrus	RH	41	-59	-13	37	7.222	.000002	147
Middle occipital gyrus	RH	28	-89	2	18	4.631	.000277	32
Inferior occipital gyrus	RH	27	-87	-9	18	5.547	.000044	47
Cuneus	RH	8	-90	11	18	4.235	.000631	18
Middle occipital gyrus	RH	36	-76	9	19	4.616	.000286	39
Inferior occipital gyrus	LH	-12	-90	-10	17	8.011	.000001	1189
Precuneus	LH	-20	-58	55	7	4.441	.000411	122
Superior Frontal gyrus	LH	-6	51	29	9	6.979	.000003	151
Precuneus	LH	-24	-71	21	31	4.608	.000291	74
Parahippocampal gyrus	LH	-21	-52	5	30	4.706	.000238	48
Superior frontal gyrus	LH	-20	10	55	6	4.732	.000226	37
Posterior cingulate	LH	-6	-50	19	30	4.238	.000627	56
Precentral gyrus	LH	-29	-9	48	6	4.762	.000212	90
Superior frontal gyrus	LH	-9	62	16	10	4.774	.000207	18

*p* < .01 (uncorrected) with an extended cluster size of 25. Bodies are presented with a grey oval, and the control stimulus is a grey oval and rectangle.

726

**Table 4** Fearful versus happy body regardless of the facial information

	Hemisphere	Talairach coordinates			Brodmann	<i>t</i>	<i>p</i>	Number of vertices
		x	y	z				
<i>Controls</i>								
Happy > Fear								
Temporal pole	RH	38	-3	-30	21	-3.636	.002225	42
Superior temporal gyrus	RH	49	9	-9	38	-2.919	.010028	39
Inferior temporal gyrus	LH	-50	-16	-25	20	-3.182	.005790	30
<i>UWD</i>								
No significant clusters								
<i>UWD and Controls</i>								
No significant clusters								

*p* < .01 (uncorrected) with an extended cluster size of 25. <sup>b</sup> did not survive cluster-size correction

727

728

729

**Table 5** Incongruent versus congruent face body compounds

	Hemisphere	Talairach coordinates			Brodmann	<i>t</i>	<i>p</i>	Number of vertices
		x	y	z				
<i>Controls</i>								
Congruent > Incongruent								
Superior frontal gyrus	RH	9	26	54	6	-3.996	.001040	30
Ventromedial prefrontal cortex	RH	8	41	-1	10	-2.414	.028110	34
<i>UWD</i>								
Congruent > Incongruent								
Insula	RH	36	-8	6	13	-3.093	.006981	46
Insula	LH	-34	-4	3	13	-2.608	.019014	51
<i>UWD and Controls</i>								
Inferior parietal lobule	LH	-32	-46	37	40	-5.817	.000026	68

*p* < .01 (uncorrected) with an extended cluster size of 25.

730

**Table 6** Task-irrelevant fear versus task-irrelevant happiness

	Hemisphere	Talairach coordinates			Brodmann	<i>t</i>	<i>p</i>	Number of vertices
		x	y	z				
<i>Controls<sup>a</sup></i>								
Task-irrelevant fear > task-irrelevant happy								
Cingulate gyrus	RH	2	-12	27	23	6.603	.000006	47
Cuneus	LH	-3	-71	13	18	2.964	.009131	25
<i>UWD<sup>a</sup></i>								
Task-irrelevant fear > task-irrelevant happiness								
Cingulate gyrus	RH	4	-10	37	24	6.741	.000005	58
Task-irrelevant happiness > task-irrelevant fear								
Middle frontal gyrus	LH	-41	16	26	46	-3.000	.008479	33
<i>UWD and Controls<sup>a</sup></i>								
Task-irrelevant fear > task-irrelevant happiness								
Cingulate gyrus	RH	4	-10	37	24	6.741	.000005	50
Cingulate gyrus	RH	2	-12	27	23	6.603	.000006	51
<i>UWD versus Controls</i>								
No significant clusters								

<sup>a</sup>*p* < .01 (uncorrected) with an extended cluster size of 25.

731

732

**Table 7** Outcome of main between-group functional activation analyses

	Hemisphere	Talairach coordinates			Brodmann	<i>t</i>	<i>p</i>	Number of vertices
		<i>x</i>	<i>y</i>	<i>z</i>				
<i>Fearful versus happy body regardless of the facial information</i>								
<i>UWD &gt; Controls</i>								
Anterior inferior parietal lobule	RH	54	-29	32	40	4.606	.000343	93
<i>Controls &gt; UWD</i>								
Fusiform gyrus	LH	-41	-69	-12	19	-4.731	.000268	33
<i>Incongruent versus congruent face body compounds</i>								
<i>UWD &gt; Controls</i>								
Medial orbitofrontal cortex	RH	14	45	-12	11	4.724	.000271	52
Ventromedial prefrontal cortex	RH	9	56	10	10	4.474	.000446	51
Dorsal medial prefrontal cortex	RH	10	38	29	9	4.641	.000320	42
<i>Controls &gt; UWD</i>								
Temporal pole	RH	40	-4	-31	21	-4.486	.000435	77
Temporal pole	LH	-33	6	-20	38	-4.430	.000487	110

All clusters survive cluster-size correction except the anterior inferior parietal lobule and fusiform gyrus.

**Table 8** Outcome of between-group effective connectivity analyses

	Hemisphere	Talairach coordinates			Brodmann	<i>t</i>	<i>p</i>	Number of vertices
		<i>x</i>	<i>y</i>	<i>z</i>				
<i>Fearful versus happy body regardless of the facial information</i>								
Seed: Inferior parietal lobule								
UWD > Controls								
Subgenual anterior cingulate	RH	8	35	1	24	4.974	.000167	50
Seed: Fusiform gyrus								
Anterior inferior parietal lobule*	LH	-54	-43	25	40	4.926	.000183	51
<i>Incongruent versus congruent face body compounds</i>								
Seed: Medial orbitofrontal cortex								
Control > UWD								
Posterior inferior parietal lobule	RH	40	-61	42	7	-4.648	.000316	58
Seed: Ventromedial prefrontal cortex								
UWD > Controls								
Precuneus	RH	7	-69	23	31	5.646	.000047	21
Cuneus	RH	8	-82	26	19	4.650	.000314	22
Seed: Dorsal medial prefrontal cortex								
UWD > Controls								
Ventromedial prefrontal cortex	LH	-6	52	12	10	5.509	.000060	29
Controls > UWD								
Superior temporal gyrus	LH	-47	20	3	22	-5.986	.000025	108
Temporal pole	LH	-40	8	-25	38	-4.486	.000435	43
Seed: Right temporal pole								
UWD > Controls								
Inferior temporal gyrus	RH	55	-22	-17	20	5.564	.000054	55
Middle temporal gyrus	RH	60	-25	-2	21	4.654	.000312	88
Middle temporal gyrus	LH	-54	-36	-1	22	4.076	.000994	37
Seed: Left temporal pole								
Controls > UWD								
Medial orbitofrontal cortex	RH	11	41	-12	11	-5.356	.000080	36
Superior frontal gyrus	RH	19	26	52	6	-5.475	.000064	38

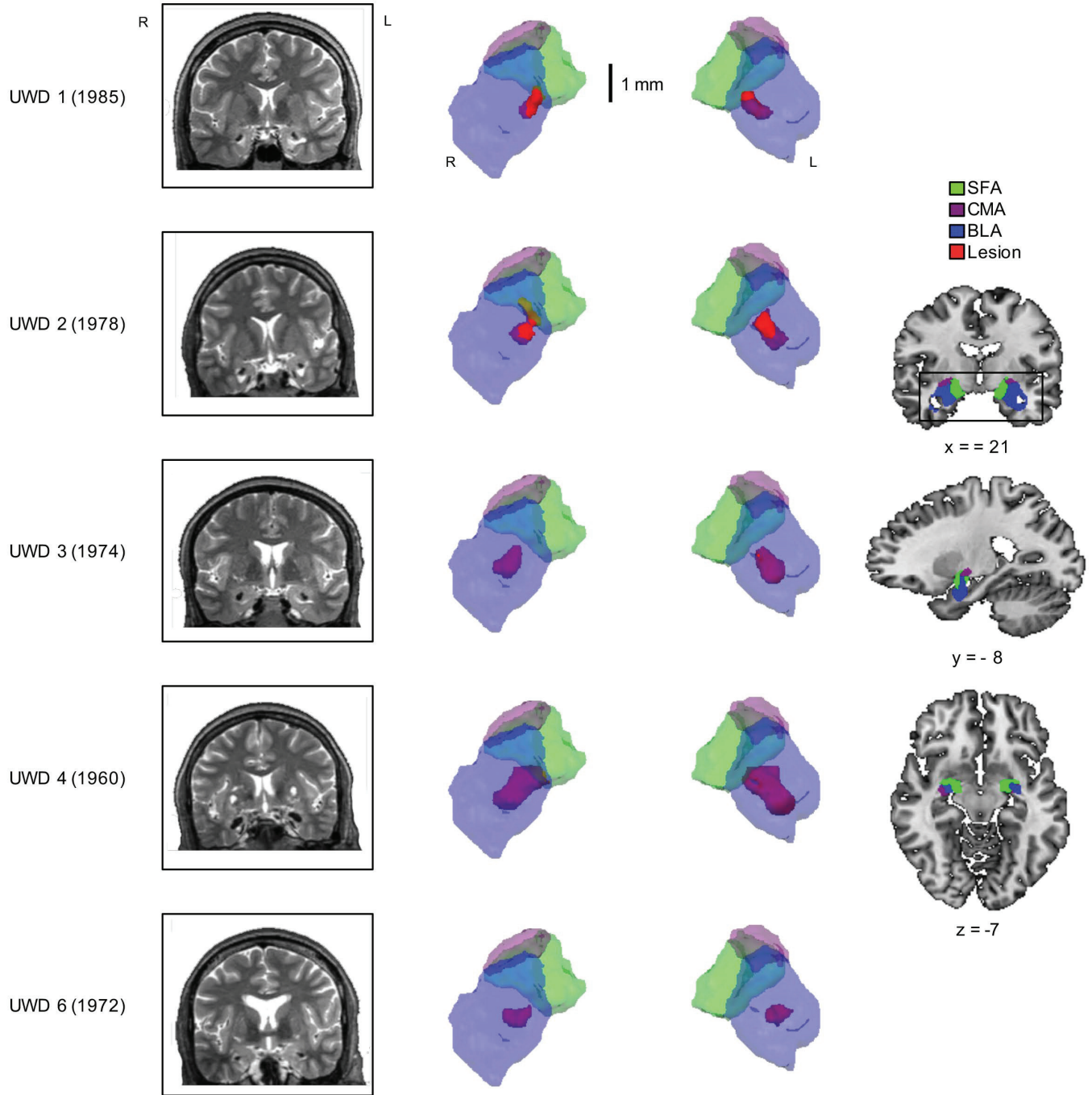
\*Did not survive cluster-size correction

734

735

736

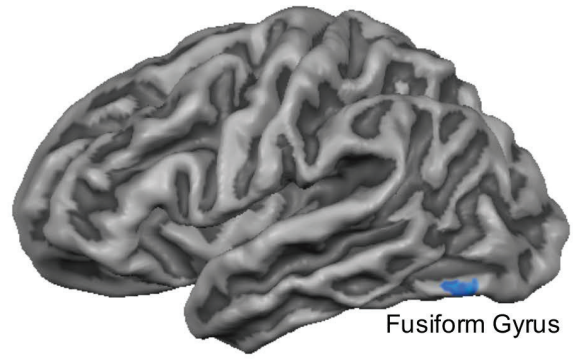
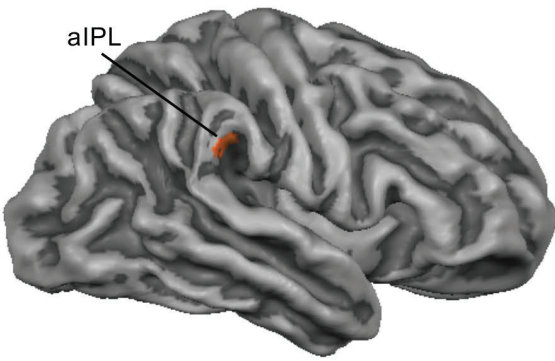
737



Fearful bodies > Happy bodies

UWD > Controls

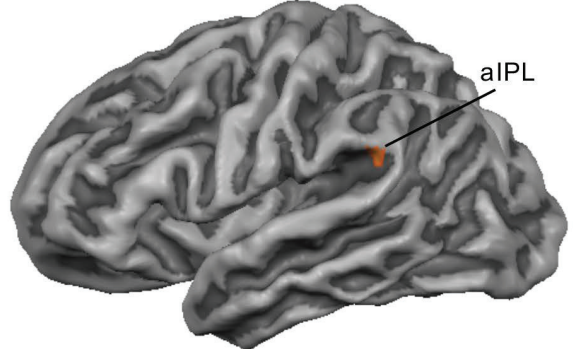
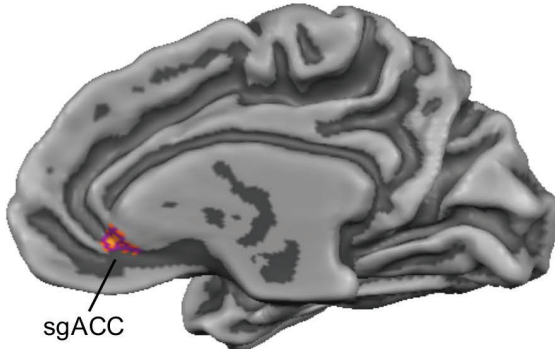
Controls > UWDs



Seed: aIPL

Seed: Fusiform Gyrus

Connectivity



UWD > Controls

UWD > Controls

